Article

Not peer-reviewed version

$CopG_1$, a Novel Transcriptional Regulator Affecting Symbiosis in *Bradyrhizobium* sp. SUTN9-2

Praneet Wangthaisong , Pongdet Piromyou , Pongpan Songwattana , Tarnee Phimphong , Apisit Songsaeng , Natcha Pruksametanan , Pakpoom Boonchuen , Jenjira Wongdee , Kamonluck Teamtaisong , Panlada Tittabutr , Nantakorn Boonkerd , Shusei Sato , Neung Teaumroong *

Posted Date: 8 May 2024

doi: 10.20944/preprints202405.0436.v1

Keywords: Symbiosis; Vigna radiata; T4SS; copG

Article

CopG1, a Novel Transcriptional Regulator Affecting Symbiosis in *Bradyrhizobium* sp. SUTN9-2

Praneet Wangthaisong [1], Pongdet Piromyou [2], Pongpan Songwattana [2], Tarnee Phimphong [1], Apisit Songsaeng [1], Natcha Pruksametanan [1], Pakpoom Boonchuen [1], Jenjira Wongdee [2], Kamonluck Teamtaisong [3], Panlada Tittabutr [1], Nantakorn Boonkerd [1], Shusei Sato [4] and Neung Teaumroong [1,*]

[1] School of Biotechnology, Institute of Agricultural Technology, Suranaree University of Technology, Nakhon Ratchasima 30000, Thailand
[2] Institute of Research and Development, Suranaree University of Technology, Nakhon Ratchasima 30000, Thailand
[3] The Center for Scientific and Technological Equipment, Suranaree University of Technology, Nakhon Ratchasima 30000, Thailand
[4] Graduate School of Life Sciences, Tohoku University, Sendai 980-8577, Japan
* Correspondence: neung@sut.ac.th

Abstract: The symbiotic interaction between leguminous and Bradyrhizobium sp. SUTN9-2 mainly relies on the nodulation process through Nod factors (NFs), while the type IV secretion system (T4SS) acts as an alternative pathway in this symbiosis. Two copies of T4SS (T4SS1 and T4SS2) are located on the chromosome of SUTN9-2. ⊗T4SS1 reduces both nodule number and nitrogenase activity in all SUTN9-2 nodulating legumes. The functions of three selected genes (copG1, traG1, and virD21) within the region of the T4SS1 were examined. We generated deleted mutants and tested in Vigna radiata cv. SUT4. ΔtraG1 and ΔvirD21 exhibited lower invasion efficiency at the early stages of root infection but could be lately restored. In contrast, ΔcopG1 completely hindered nodule organogenesis and nitrogenase activity in all tested legumes. ΔcopG1 showed low expression of nodulation gene and ttsI, but exhibited high expression levels of T4SS genes, traG1 and trbE1. The secreted proteins from ΔT4SS1 were down-regulated compared to the wild type. Although ΔcopG1 secreted several proteins after flavonoid induction, T3SS (nopP and nopX) and C4-dicarboxylate transporter (dct) were not detected. These results confirm the crucial role of the copG1 gene as a novel key regulator in the symbiotic relationship between SUTN9-2 and legumes.

Keywords: symbiosis; *Vigna radiata*; T4SS; *copG*

1. Introduction

A complex exchange of signals between legumes and rhizobia bacteria is the key factor in the successful symbiosis between two partners. The establishment of nitrogen-fixing nodules is ensured by this intricate communication system, which is crucial for legumes to thrive in nitrogen-limited environments [1,2]. Two crucial mechanisms are necessary for the nodulation process of many rhizobia: (i) the classical mechanism of perception of the Nod factor (NF) and (ii) the type III secretion system (T3SS) which deliver effector proteins into plant cells [3,4]. NFs are well-studied while, we are just beginning to understand the roles of effectors/secretion systems. The secreted effector proteins from T3SS (T3Es) can have either a positive or negative impact on the symbiosis efficiency, depending on the plant species [5]. For example, *Bradyrhizobium vignae* ORS3257 contains multiple effector proteins crucial for modulating symbiotic properties in different *Vigna* species. NopT and NopAB play essential roles in nodulation in *V. unguiculata* and *V. mungo*. Whereas, NopP2 displayed incompatibility with *V. radiata* [6]. Beside the T3SS, others secretion systems have been identified in several rhizobia genera, including type IV and VI secretion systems (T4SS and T6SS) and these systems have also reported as the key determinant to the symbiotic interactions during infection processes. For instance, the T6SS of *Rhizobium etli* Mim1 and *Bradyrhizobium* sp. LmicA16 (A16)

 doi:10.20944/preprints202405.0436.v1

exhibit a positive effect on nodulation with their host [8,9]. In the case of T4SS, this secretion machinery is found in various bacteria, including *Rhizobium*. It functions as a molecular channel, allowing bacteria to transport diverse molecules across their cell envelope [10]. Various rhizobia, including *Bradyrhizobium*, *Rhizobium*, *Sinorhizobium*, and *Mesorhizobium*, possess T4SS which belongs to the *tra/trb* operon and could be found either in chromosome or plasmid depending on the bacterial strain [11–14]. Interestingly, most of bradyrhizobia harbor the *tra/trb* operon on the chromosome. Few studies about the role of T4SS of *Bradyrhizobium* in the symbiotic process have been reported. Previously, we found two clusters of T4SS (T4SS$_1$ and T4SS$_2$) located on the chromosome of *Bradyrhizobium* sp. SUTN9-2 with different gene arrangements (Figure S1). Additionally, a specialized gene arrangement consisting of *copG*, *traG*, and *virD2* genes was observed in the T4SS gene cluster of *Bradyrhizobium* species. The T4SS evolutionary analysis of the *Rhizobiales* order, encompassing *Bradyrhizobium*, *Rhizobium*, *Sinorhizobium*, and *Mesorhizobium* through the *traG* gene phylogenetic tree, demonstrates a co-evolutionary trend between *Bradyrhizobium* and *Mesorhizobium*. Upon phylogenetic examination of the *copG*, *traG*, and *virD2* combination genes in *Bradyrhizobium*, two copies of these clusters were divided into two clades within the bradyrhizobia group [15]. Moreover, copy 1 of *copG*, *traG*, and *virD2* genes exhibits a close evolutionary association with *B. yuanmingense* BRP09, which are main rhizobia associated with cowpea and mung bean in the subtropical region of China [16], as well as with *B. diazoefficiens* USDA110, soybean inoculant [17]. Interestingly, T4SS$_1$ mutant (deleted *copG*$_1$, *traG*$_1$, and *virD2*$_1$ fragment) retard nodulation in *V. radiata* cv. SUT4 and *Crotalaria juncea* and both the number of nodules and nitrogenase activity were decreased compared with the wild type. The results indicated that T4SS$_1$ has a positive effect on the symbiotic interaction with tested plants [15]. To understand the role of T4SS$_1$ in the symbiotic process, individual deletion mutants were generated in *copG*$_1$, *traG*$_1$ and *virD2*$_1$ genes (encoding a putative transcriptional factor gene, T4SS structural gene, and relaxase gene, respectively), and examined for their roles in the symbiotic interaction with *V. radiata* cv. SUT4 [18–20]. In addition to *V. radiata* cv. SUT4, the loss of nodulation ability was observed in different plant species of Genistoids, Dalbergioids, and Millettioids upon infection with Δ*copG*$_1$ (Table S1).

2. Materials and Methods

2.1. Bacterial Strains, Plasmids, and Growth Conditions

The bacterial strains and plasmids used in this study are listed in Table 1. *Bradyrhizobium* sp. SUTN9-2 was grown in arabinose-gluconate (AG) medium [21]. The derivative mutants Δ*copG*$_1$, Δ*traG*$_1$, and Δ*virD2*$_1$ were supplemented with streptomycin (sm) at 200 µg/mL. *Escherichia coli* strains were grown at 37°C in Luria–Bertani (LB) medium. Antibiotic was added in to the medium as required at the following concentrations: 50 µg/mL kanamycin (km), 30 µg/mL nalidixic acid (nal), and 200 µg/mL streptomycin (sm).

Table 1. Bacterial strains and plasmids used in this study.

Strain or plasmid	Relevant characteristics	Reference or source
Strain		
Bradyrhizobium sp. SUTN9-2	*A. americana* nodule isolate (paddy crop)	
Δ*copG*$_1$	SUTN9-2 derivative containing an Ω cassette insertion at *HindIII* site, *copG* copy 1::sm/sp; Sm^r, Sp^r	This study
Δ*copG*$_2$	SUTN9-2 derivative containing an Ω cassette insertion at *BamHI* site, *copG* copy 2::sm/sp; Sm^r, Sp^r	This study
Δ*traG*$_1$	SUTN9-2 derivative containing an Ω cassette insertion at *BamHI* site, *traG* copy 1::sm/sp; Sm^r, Sp^r	This study
Δ*virD2*$_1$	SUTN9-2 derivative containing an Ω cassette insertion at *BamHI* site, *virD2* copy 1::sm/sp; Sm^r, Sp^r	This study

 doi:10.20944/preprints202405.0436.v1

Escherichia coli DH5α	*supE44 ΔlacU169 hsdR17 recA1 endA1 gyrA96 thi-1 relA1*	Toyobo Inc.
Plasmid		
pRK2013	ColE1 replicon carrying *RK2* transfer genes; Km^r; Helper plasmid	[22]
pNTPS129	Cloning vector harboring *sacB* gene under the control of the constitutive *npt2* promoter; Km^r	[23]
pNTPS129-Δ*copG*$_1$	pNTPS129-*npt2*-*sacB* containing the flanking region of *copG* copy 1	This study
pNTPS129-Δ*copG*$_2$	pNTPS129-*npt2*-*sacB* containing the flanking region of *copG* copy 2	This study
pNTPS129-Δ*traG*$_1$	pNTPS129-*npt2*-*sacB* containing the flanking region of *traG* copy 1	This study
pNTPS129-Δ*virD2*$_1$	pNTPS129-*npt2*-*sacB* containing the flanking region of *virD2* copy 1	This study

2.2. Plasmid Construction and Gene Deletion

The deletion mutants of *copG*$_1$, *copG*$_2$, *traG*$_1$, and *virD2*$_1$ genes in *Bradyrhizobium* sp. SUTN9-2 (GeneBank accession number LAXE00000001) were obtained as follows. The upstream and downstream regions of *copG*$_1$ (up: 575 bp, dw: 841 bp), *copG*$_2$ (up: 874 bp, dw:1043 bp), *traG*$_1$ (up: 1060 bp, dw:921 bp), and *virD2*$_1$ (up: 944 bp, dw: 738 bp) genes were obtained by PCR using primers listed in Table 2. The target deletion genes in SUTN9-2 were obtained by double crossover. PCR fragments corresponding to the upstream and downstream flanking regions of the gene of interest were merged by overlap extension and introduced into a pNTPS129 plasmid harboring the *sacB* gene [23]. Then, an Ω cassette fragment (spectinomycin/streptomycin resistance genes) from pHP45 (omega) [24] was introduced between upstream and downstream flanking regions which were already cloned into pNTPS129. The restriction site for antibiotic insertion was *HindIII* for *copG*$_1$ and *BamHI* for *copG*$_2$, *traG*$_1$, and *virD2*$_1$. The resulting plasmids were transferred into SUTN9-2 by triparental mating using pRK2013 as a helper plasmid [22] as described previously [15]. A single recombinant clone was obtained by antibiotic selection and PCR verification. Double recombinant clones were selected by culture on AG medium supplemented with 10% sucrose and 200 μg/mL sm. Candidate clones were verified for the loss of the *sacB* gene from pNTPS129, and the replacement of the Ω cassette was verified by PCR. All mutant strains were further investigated for nodulation efficiency in *V. radiata* cv. SUT4.

Table 2. Primers used in this study.

Name	Sequences (5′-3′)	Descriptions
Primers for gene deletion		
Up.*copG*$_1$.*XbaI*.F	CCT TGA GAT CTA GAT GTA GTC TGC CCC GAA GTA GC	This primer sets used to obtain the deletion of *copG*$_1$ gene of *Bradyrhizobium* sp. SUTN9-2 by double crossing over.
Up. *copG*$_1$. overl. *HindIII*. R	GAG GCG GAC ATG AAA GCT TAA TGA AGG CGG ACG GCC ACT AG	
Dw. *copG*$_1$. overl. *HindIII*. F	GTC CGC CTT CAT TAA GCT TTC ATG TCC GCC TCA CAG TCC GA	
Dw. *copG*$_1$. *EcoRI*.R	AGA TCG GGA ATT CGT TGA CCG AGG ATC TTC AGG CCA	
Up. *copG*$_2$. *XbaI*.F	GCC GTT TCT AGA ATT GCG ACA ACG GAC CAG GGC AA	

 doi:10.20944/preprints202405.0436.v1

Up. *copG*$_2$. overl. *HindIII*. R	GCG CGA CCG AAT GAA GCT TAA GCT GGT CAC GCT ATC GGC T	This primer sets used to obtain the deletion of *copG*$_2$ gene of *Bradyrhizobium* sp. SUTN9-2 by double crossing over.
Dw. *copG*$_2$. overl. *HindIII*. F	GCG TGA CCA GCT TAA GCT TCA TTC GGT CGC GCA TAT TGC C	
Dw. *copG*$_2$. *EcoRI*. R	CTG TCC GAA TTC ATG TCG TTC CTC GGG TTG TAC C	
Up. *traG*$_1$. *XbaI*. F	TTC GGG TCT AGA TGT AGT CTG CCC CGA AGT AGC	This primer sets used to obtain the deletion of *traG*$_1$ gene of *Bradyrhizobium* sp. SUTN9-2 by double crossing over.
Up. *traG*$_1$. overl. *BamHI*	TCC CTC CAA TCA CGG ATC CAT CCT GGT GAC GAT CTC GGA C	
Dw. *traG*$_1$. overl. *BamHI*	TCG TCA CCA GGA TGG ATC CGT GAT TGG AGG GAT CGT TCA CAG	
Dw. *traG*$_1$.*EcoRI*.R	CCG GCT GAA TTC CTT GGA AAG CCT TGG TCT CG	
Up. *virD2*$_1$. XbaI. F	ACC GGC TTC TAG AAG ATG CGC AGT CCG CAT CAT C	This primer sets used to obtain the deletion of *virD2*$_1$ gene of *Bradyrhizobium* sp. SUTN9-2 by double crossing over.
Up. *virD2*$_1$. overl. *BamHI*	GAG GAG AAG GAA TGG ATC CTG AAC GAT CCC TCC AAT CAC CG	
Dw. *virD2*$_1$. overl. *BamHI*	GAG GGA TCG TTC AGG ATC CAT TCC TTC TCC TCA GCC ATG GC	
Dw. *virD2*$_1$. *EcoRI*. R	CCA TCG GAA TTC TTG TCG ATG CGG AGG AGG CAT C	
Primers for qRT-PCR analysis		
SUTN9-2. *nodA*. F	GTT CAA TGC GCA GCC CTT TGA G	Specific primers for *nodA* gene expression in SUTN9-2 on chromosome
SUTN9-2. *nodA*. R	ATT CCG AGT CCT TCG AGA TCC G	
SUTN9-2. *nodC*. F	ATT GGC TCG CGT GCA ACG AAG A	Specific primers for *nodC* gene expression in SUTN9-2 on chromosome
SUTN9-2. *nodC*. R	AAT CAC TCG GCT TCC CAC GGA A	
SUTN9-2. *nodD1*. F	ATT CGT CTC CTC AGA CCG TGC T	Specific primers for *nodD1* gene expression in SUTN9-2 on chromosome
SUTN9-2. *nodD1*. R	TTC ATG TCG AGT GCG CAC CCT A	
SUTN9-2. *nodD2*. F	TGC TTA ACT GCA ACG TGA CCC	Specific primers for *nodD2* gene expression in SUTN9-2 on chromosome
SUTN9-2. *nodD2*. R	ATG AGC ACG AGG AGC TTC TC	
SUTN9-2. *trbE*$_1$. F	GAT TGC AGG AGA ACC GTG AGG C	Specific primers for *trbE*$_1$ gene expression in SUTN9-2 on chromosome
SUTN9-2. *trbE*$_1$. R	AAC AGC GCC GAG GAT TCA GTC T	

 doi:10.20944/preprints202405.0436.v1

SUTN9-2. *traG*$_1$. F	TTC TCG ATC TGG TTC AGC GAC TG	Specific primers for *traG*$_1$ gene expression in SUTN9-2 on chromosome
SUTN9-2. *traG*$_1$. R	TTG ACC GAG GAT CTT CAG GCC A	
SUTN9-2. *ttsI*. F	ATG AGT TCG TCG GTG GAC AC	Specific primers for transcriptional regulator TtsI (*ttsI*) gene expression in SUTN9-2 on chromosome
SUTN9-2. *ttsI*. R	CCA CAT GGT CCT GCT CGA AT	
16s. F	ATT ACC GCG GCT GCT GG	Universal primers for 16S rRNA used as internal control for bacterial gene expression [25]
16s. R	ACT CCT ACG CGA GGC AGC AG	
dct. F	CGA CTA TCA GGG CGT GAA AT	Specific primers for C$_4$-dicarboxylate transport (*dct*) gene expression in SUTN9-2 on chromosome
dct. R	TCC AGC AAT CAG ACC TGT G	
nopX. F	GGGTGGTCGAGGAAGTATTG	Specific primers for Type III secretion system (T3SS) gene expression in SUTN9-2 on chromosome
nopX. R	GGTTATGACCCAGACCGATG	
nopP. F	GGTCACACCGACGAAGATAC	
nopP. R	CCGAAGATCCACTTGGGATG	

2.3. Nodulation Test and Acetylene Reduction Assay (ARA)

V. radiata cv. SUT4 seeds were surface-sterilized and germinated as previously described [26] and placed on 0.85% water agar at 28°C overnight. One-day-old germinated seedlings were transferred into Leonard's jars containing sterilized vermiculite and liquid buffered nodulation media (BNM) [27]. At seven days after gemination, seedlings were inoculated with a bacterial suspension of *Bradyrhizobium* sp. SUTN9-2 or derivative mutants (1 ml per seedling; adjusted to OD_{600} = 0.8). Five plants per treatment were selected for nodule counting. The symbiotic phenotypes and nitrogen activity were measured at 7, 14, and 21 dpi.

Acetylene reduction assays (ARAs) were used to evaluate the nitrogenase activity. The root samples were transferred into test tubes, which were closed with a plastic stopper. Then, the samples were incubated with 10% (v/v) pure acetylene instead of air, which was withdrawn for 1 h at room temperature. A 1 ml sample was examined using gas chromatography (GC) with a PE-alumina-packed column to measure the conversion of acetylene (C_2H_2) to ethylene (C_2H_4). Detection was done at an injection temperature of 150°C and oven temperatures of 200°C and 50°C for flame ionization detection (FID) [28]. The experiment was conducted with five biological replicates per treatment. The nitrogenase activity is presented in nmol ethylene/h/plant dry weight [29].

The symbiotic profiles of Δ*copG*$_1$ were compared to SUTN9-2 using a growth pouch test and several leguminous plants, including Genistoids (*Crotalaria juncea*), Dalbergioids (*Aeschynomene americana* cv. Thai, *Arachis hypogaea* cv. Thainan 9 and *A. hypogaea* cv. Khonkaen 5), and Millettioids (*Indigofera tinctoria*, *Macroptilium atropurpureum*, *V. radiata* cv. SUT1, *V. radiata* cv. CN72, *V. radiata* cv. KUML4, *V. radiata* cv. CN36, *V. radiata* cv. KPS1, *V. mungo* cv. U thong 2 and, *V. subterranean*). Seeds were surface-sterilized and germinated as previously described [26,30]. Pouches were prepared [29] and supplemented with BNM medium. Seedlings were grown at two plants per pouch (Five pouch replicates per treatment) and inoculated with 1 ml per plant of a suspension containing OD_{600} = 0.8. Plants were grown under the conditions mentioned above.

2.4. Bacterial Induction, RNA Isolation, and qRT-PCR Analysis of Gene Expression

For bacterial induction, the mid-log phase of bacteria cultures including *Bradyrhizobium* sp. SUTN9-2 and *copG*$_1$ mutant strains (OD_{600} = 0.4) were induced by 20 µM genistein at 28°C for 24 hours. Then, bacterial pellets were collected by centrifugation (4,000×g, at 4°C) for total RNA isolation. Total RNA was isolated from bacterial pellets using an RNeasy® Protect Cell Mini Kit (Qiagen,

 doi:10.20944/preprints202405.0436.v1

Chatsworth, CA, U.S.A.) according to the manufacturer's instructions. Total RNA was treated at 37°C for 30 min with RNase-free DNase I (NEB, USA).

cDNA was synthesized using iScript™ Reverse Transcription Supermix for RT-qPCR (Bio-Rad Laboratories, Inc.) according to the manufacturers' protocols. A cDNA concentration of 50 ng/µL was subjected to real-time PCR using specific primers (Table 2) for nodulation genes (*nodA*, *nodB*, *nodC*, *nodD1*, and *nodD2)*, transcriptional regulator of T3SS (*ttsI*), T4SS structural genes (*traG*$_1$ and *trbE*$_1$), and other genes. qRT-PCR reactions were performed with Luna® Universal qPCR Master Mix (NEB, USA) by following the manufacturer's protocol, and thermal cycling was conducted in a CFX Opus 96 Real-Time PCR System (Bio-Rad Laboratories, Inc.). The reactions were done in triplicate for each of the three biological replicates. Relative gene expression was analyzed by the comparative Ct method 2(-ΔΔCT), and 16s rRNA (accession number: JN578804) was used as internal control [11]. Three biological replicates were analyzed.

2.5. Protein Preparation, Sodium Dodecyl Sulfate Polyacrylamide Gel Electrophoresis (SDS-PAGE) Analysis, and Protein Identification

Wild type (WT) and Δ*copG*$_1$ *Bradyrhizobium* sp. SUTN9-2 were grown in AG medium with shaking at 200 rpm and 30°C until they reached an OD_{600} of 1. One percent (v/v) of each starter was inoculated into 100 ml of AG medium with and without 20 µM genistein induction. Then, cultures were incubated at 30°C until they reached an OD_{600} of approximately 1.0. The bacterial supernatants were harvested by centrifugation at 4,000xg and 4°C for 1 h, followed by 8,000xg for 30 min. One milliliter of 1 M dithiothreitol (DTT) and 7.5 ml of phenol solution (equilibrated with 10 mM Tris HCl at pH 8.0 with ESTA) were added into 25 ml of fresh supernatant. The solution was vigorously mixed with a vortex before centrifugation at 8,000xg and 4°C for 30 min. The water phase was discarded, and the phenol phase was added into another 25 ml of supernatant, followed by vigorous mixing and centrifugation at 8,000xg and 4°C for 30 min. Next, 20 ml of methanol containing 300 µl of 8 M ammonium acetate and 400 µl of 1 M dithiothreitol were added to remove the phenol phase. The secreted protein was precipitated for overnight at -20°C. The solution was then centrifuged at 8,000xg and 4°C for 1 h, and the supernatant was discarded. After precipitation, the protein was washed with chilled 70% (v/v) ethanol and air-dried in a laminar flow before being dissolved in phosphate-buffered saline (PBS). Protein concentrations were determined using a plate reader and the manufacturer's protocol (PanReac) according to the method of Bradford [31]. A standard calibration curve was constructed using 0 to 2 µg of bovine serum albumin (BSA). Denaturing SDS-PAGE was carried out according to the method of Laemmli [32], in which 10 µg each lane of protein were analyzed on a 12% SDS-PAGE gel. The protein samples were mixed with loading buffer containing β-mercaptoethanol and heated for 10 min before loading. Protein bands were stained with colloidal Coomassie brilliant blue R-250 for visualization of the expression of secreted protein. The protein bands which were observed on WT lane but not observed on ΔT4SS$_1$ lane were cut protein identification by mass spectrometry. Breiftly, the protein bands were performed in-gel digestion by 12.5 ng/µL trypsin (mass spectrometry grade; Promega, USA). The extacted peptides were collected and dried in the Nitrogen Evaporator (Organomation, USA). Then, the peptide were reconstituted in 15 µl of 0.1% formic acid (FA) for LC/MS analysis. The LC–MS/MS system consists of a liquid chromatography part (Dionex Ultimate 3000, RSLCnano System) in combination with an captivespray ionization / mass spectrometer (Model Q-ToF Compact, Bruker, Germany) at the Proteomics Services, Faculty of Medical Technology, Mahidol University (Salaya Campus), Nakonpathum, Thailand. Mass spectral data from 300 to 1500 m/z was collected in the positive ionization mode. The most abundant peptide ions were analysed using MS/MS, to determine the peptide sequence. The peptide sequence was searched on the Uniprot database using the Mascot daemon version 2.6.0 (Matrix Science, London, UK) searching engine. The search parameters in Mascot daemon MS/MS Ions search included carbamidomethyl at cysteine residues as a fixed modification and oxidation on methionine as variable modifications. The peptide tolerance was set at ±1.6 Da, and the MS/MS fragment tolerance was set at ±0.8 Da. Protein hits were selected with a p-

 doi:10.20944/preprints202405.0436.v1

value of ≤ 0.05. The obtained results were examined against protein-NCBI database to identify and annotate proteins.

2.6. Microscopy

The nodule phenotypes and cross sections of representative nodules generated by the wild type (WT) or mutants were examined under stereomicroscope (LEIGA EZ4). For in-situ live/dead cell staining, the nodules were harvested and embedded with 5% agarose [33]. Three plants per treatment were selected for nodule sections with thickness of 40-50 µm were prepared with a VT1000S vibratome (Leica Nanterre, France) and incubated with live/dead staining solution (5 µM SYTO9 and 30 µM propidium iodide (PI) in PBS pH 7.0 buffer) for 30 min, followed by staining with 1X calcofluor white stain for 20 min. Sections were washed to remove the staining solution and mounted in 10% glycerol in 1X PBS buffer. After staining, nodules were observed by confocal microscopy using a Nikon Inverted Eclipse Ti-E Confocal Laser Scanning Microscope. Calcofluor was detected with emission at 460-500 nm, while SYTO9 and PI were detected at 510-570 nm and 600-650 nm, respectively [15]. Three nodules were randomly selected for nodule imaging and bacteroid observation.

2.7. Bioinformatics

Bradyrhizobium sp. SUTN9-2 genome sequences were obtained from the NCBI database (https://www.ncbi.nlm.nih.gov) and Genoscope (https://mage.genoscope.cns.fr) [35]. Multiple sequence alignments were determined by CLUSTALW (2.1) (https://www.genome.jp/tools-bin/clustalw). Domain architecture analysis was performed with the Simple Modular Architecture Research Tool (SMART) (https://smart.embl.de) [36] and InterPro (https://www.ebi.ac.uk/interpro) [37]. The annotation features and whole genome sequences were analyzed by SnapGene software (www.snapgene.com).

2.8. Statistical Analysis

All data were obtained from experiments performed in triplicate. For statistical analyses, one-way analysis of variance (ANOVA) followed by Tukey's honestly significant difference (HSD) test (Tukey's tests at $P \leq 0.05$) and Student's *t*-tests ($P \leq 0.05$) were performed using SPSS software (SPSS version 22.0 windows: SPSS Inc., Chicago, IL) and GraphPad Prism statistical software (Version 10.0.3).

3. Results

3.1. Symbiotic Properties of ΔcopG1, ΔtraG1, and ΔvirD21 in Vigna Radiata cv. SUT4 Symbiosis

Differences between the wild type and mutants of *Bradyrhizobium* sp. SUTN9-2 were observed in terms of nodulation and nitrogenase activity in *V. radiata* cv. SUT4 (Figure 1). Δ*traG*1 and Δ*virD2*1 induced a higher number of nodules on the plant tested than the wild type at 7 days post inoculation (dpi) (Figure 1Q), although the nodules produced displayed a white color (Figure 1I and 1M) instead of pink, indicating problems in nodule development. Moreover, there were higher numbers of dead cells in nodules inoculated with Δ*traG*1 and Δ*virD2*1 in the symbiosome area (Figure 1J and 1N). At 21 dpi, there was no difference in the number of nodules obtained with Δ*traG*1, Δ*virD2*1, and the wild type (Figure 1R).

In addition, there were different results of the nitrogenase activities in each mutant at 21 dpi, Δ*traG*1 was identical to that of the wild type, while low nitrogenase activity was obtained with Δ*virD2*1 (Figure 1T). Interestingly, Δ*copG*1 showed a significant effect on nodulation in that nodule formation was abolished (Figure 1E, 1G and 1Q-1R). Although nodule organogenesis was not observed in the plant inoculated with Δ*copG*1, both live and dead cells were detected in the cortex and vascular tissue instead (Figure 1H). According to the results, Δ*copG*1 was able to infect plant cells, but it was no longer capable of surviving in host cells.

 doi:10.20944/preprints202405.0436.v1

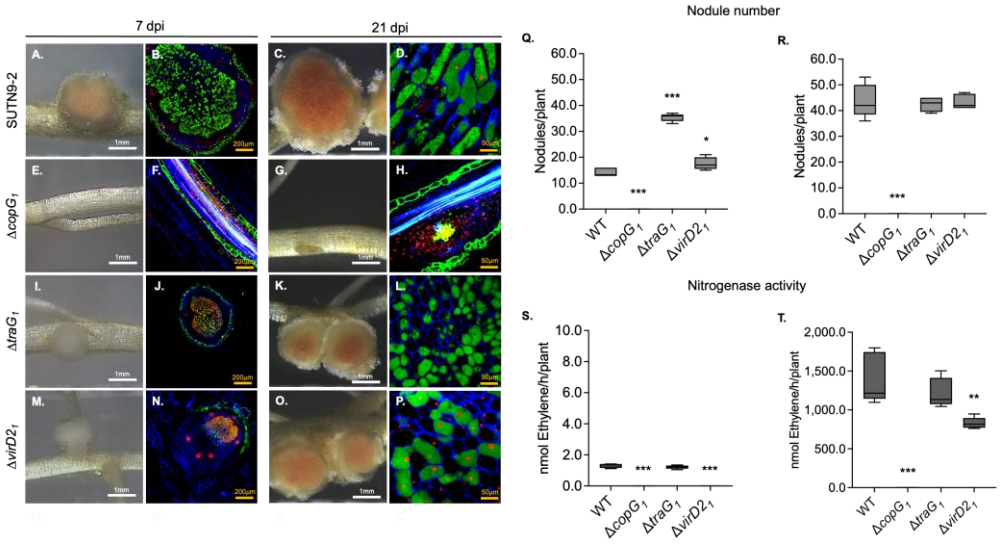

Figure 1. Symbiotic phenotype of *Bradyrhizobium* sp. SUTN9-2 mutants during symbiosis with *Vigna radiata* cv. SUT4. Nodule phenotype at 7 and 21 dpi generated by wild type (A, C), Δ*copG*$_1$ (E, G), Δ*traG*$_1$ (I, K) and Δ*virD2*$_1$ (M, O). Cytological analysis of the nodules (at 7 dpi and 21 dpi) induced by SUTN9-2 with wild type (B, D), Δ*copG*$_1$ (F, H), Δ*traG*$_1$ (J, L) and Δ*virD2*$_1$ (N, P) observed by confocal microscopy after staining with propidium iodide, PI (red; infected plant nuclei and dead bacteria), SYTO9 (green: live bacteria), and calcofluor (blue: plant cell wall). Number of nodules at 7 dpi (Q) and 21 dpi (R). Nitrogen fixation activity determined by the acetylene reduction assay (ARA) of plants infected with the indicated bacterial mutants at 7 dpi (S) and 21 dpi (T). Values represent mean ± SD (n = 5). Scale bars; white bars indicate 1 mm, yellow bars indicate 100 µm (20X) and 50 µm (40X). *P* values based on Tukey's test (* P <0.05,** P<0.01,*** P < 0.001).

3.2. The copG Genes Are Involved in Nodulation Efficiency of Bradyrhizobium sp. SUTN9-2

The *copG* gene typically encodes the CopG protein, which is a transcriptional factor that consists of ribbon helix-turn-helix (RHH) motifs [18,34,38]. *Bradyrhizobium* sp. SUTN9-2 has two copies of *copG* genes located downstream of the *traG* and *virD2* genes. These gene clusters are located in distinct locations on the SUTN9-2 chromosome. Although two copies of *copG* genes were present on the chromosome, they did not share the same gene sequences. The *copG* gene copies 1 and 2 (*copG*$_1$ and *copG*$_2$) revealed a low degree of similarity with 52.35% DNA sequence identity (Figure S2) and 51.77 % amino-acid sequence identity (Figure S3), which are different in both the N- and C-terminals. Domain architecture analysis identified CopG$_1$ as an unidentified domain, which shows similarities with *B. yuanmingense* BRP09, CCBAU05623, and, more distantly, in P10 130. While, CopG$_2$ was identified as a Pfam:RHH domain that is also found in *B. diazoefficiens* USDA110, *B. diazoefficiens* SEMIA5080, and *B. japonicum* J5 (Figure S4).

To gain a more complete understanding of the function of *copG*$_1$ and *copG*$_2$, we constructed Δ*copG*$_2$, inoculated it into *V. radiata* cv. SUT4, and compared it with Δ*copG*$_1$ and wild type strains (Figure 2). Contrary to Δ*copG*$_1$ (Figure 2B), Δ*copG*$_2$ was able to produce pink nodules (Figure 2C) that were smaller than those generated by the wild type (Figure 2A). At 14 and 21 dpi, Δ*copG*$_2$ produced the highest number of nodules compared to other strains (Figure 2G and 2H). Despite the high number of nodules generated by Δ*copG*$_2$, the nitrogenase activity was significantly lower than that of the wild type (Figure 2I and 2J). Confocal microscopic examination showed dead cells in nodules generated by Δ*copG*$_2$ (Figure 2F) in the symbiosome, in contrast with the wild type (Figure 2D). These findings indicated both *copG*$_1$ and *copG*$_2$ genes are essential for the symbiotic relationship between SUTN9-2 and legume plants. *copG*$_1$ is necessary for nodulation, while *copG*$_2$ is crucial for nitrogenase efficiency. Lack of *copG*$_2$ leads to decreased nitrogenase activity, despite the presence of high nodule numbers.

Preprints.org (www.preprints.org) | NOT PEER-REVIEWED | Posted: 8 May 2024 doi:10.20944/preprints202405.0436.v1

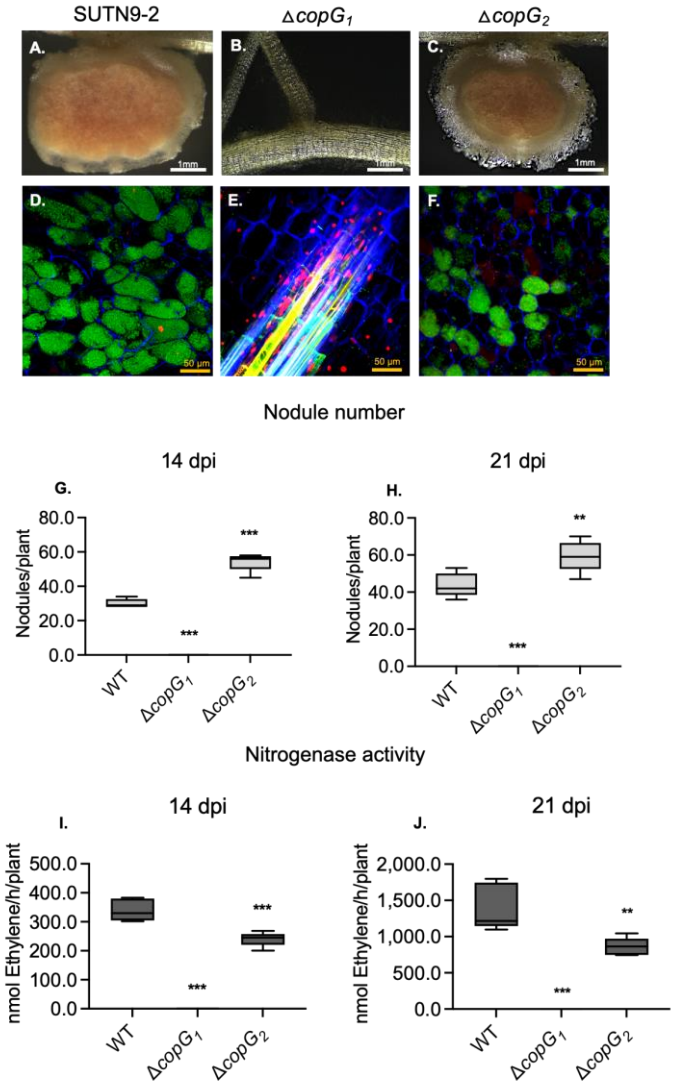

Figure 2. Derivative *copG* mutants of *Bradyrhizobium* sp. SUTN9-2 presenting different symbiotic interaction with *Vigna radiata* cv. SUT4. Nodule phenotypes induced by wild type (A), Δ*copG*1 (B), and Δ*copG*2 (C). Cytological analysis of live/dead cells of section nodule infected with wild type (D), Δ*copG*1 (E), and Δ*copG*2 (F) at 14 dpi were observed with confocal microscopy, and bacteroids were stained with PI, SYTO9, and calcofluor-white. Number of nodules at 14 dpi (G) and 21 dpi (H). Nitrogen fixation activity determined by ARA of plants infected with the indicated bacterial mutants at 14 (I) and 21 dpi (J). Values represent mean ± SD (n = 5). Scale bars; white bars indicate 1 mm and yellow bars indicate 50 µm (40X). *P* values based on Tukey's test (** *P* <0.01, *** *P* <0.001).

3.3. The copG1 Gene Plays a Crucial Role in the Expression of Nodulation (nod) Genes and Transcriptional Regulator TtsI (ttsI)

To examine if *copG*1 affects the structuring of the NF backbone, transcript levels of *nodABC* and transcriptional activator *nodD* (*nodD1* and *nodD2*) were examined with and without 20 µM genistein induction (Figure 3). The *nodA*, *nodC*, *nodD1*, and *nodD2* genes were almost not expressed in Δ*copG*1 (Figure 3A, 3C, 3D and 3E), while the expression of *nodB* was not affected by a mutation in *copG*1 (Figure 3B). The results indicated that *copG*1 modulate, either directly or indirectly, the expression of *nod* genes, especially the *nodD* gene (Figure 3D and 3E), which is a transcriptional activator of NFs [39]. Beside NF biosynthesis, NodD1 also activated the transcriptional regulator TtsI (*ttsI*), gene encoding for T3SS secretion and synthesis [40]. Similar to the *nod* genes, the expression level of *ttsI* was not determined in Δ*copG*1 in all conditions (Figure 3F). The loss of nodule formation in Δ*copG*1

 doi:10.20944/preprints202405.0436.v1

may be caused by the suppression of NF synthesis and also T3SS due to the absence of *nodD* expression.

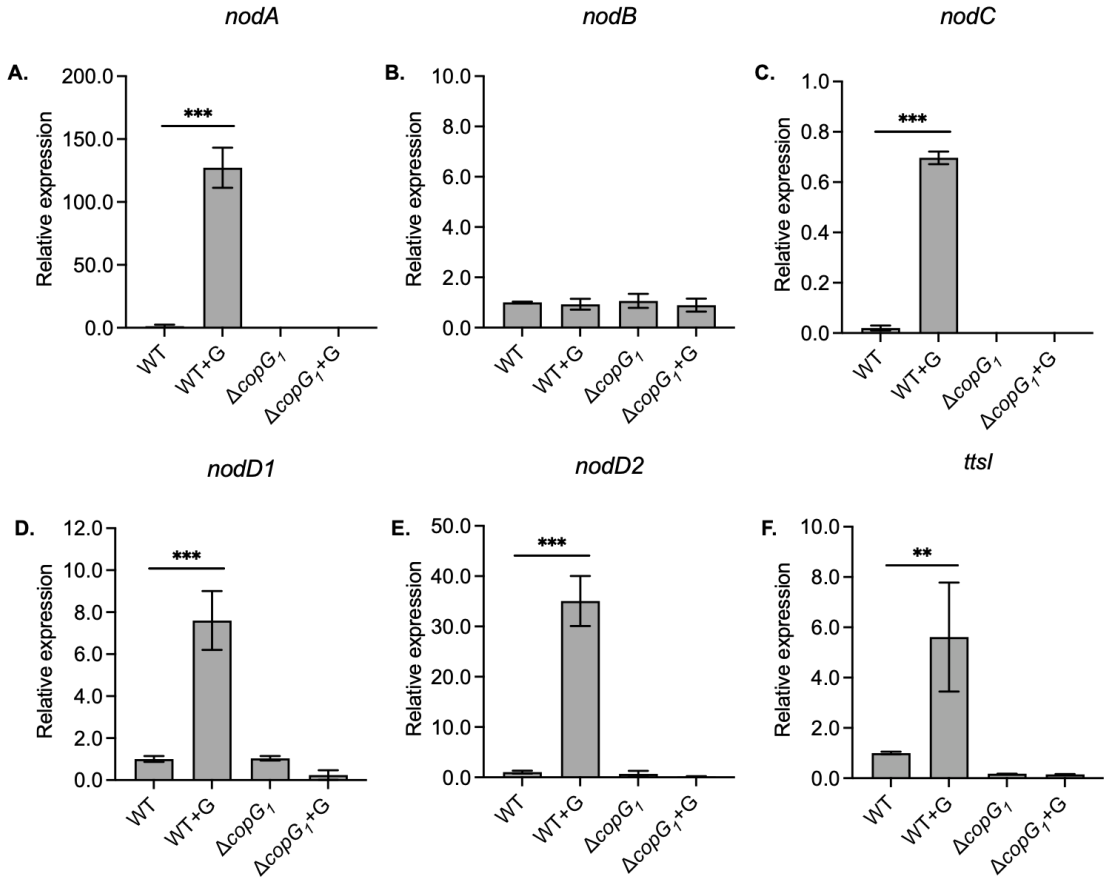

Figure 3. qRT-PCR analysis of *nod* genes from wild type *Bradyrhizobium* sp. SUTN9-2 (WT) and Δ*copG*$_1$ grown in absence and presence of 20 µM genistein (G). Expression of structural genes *nodA* (A), *nodB* (B), and *nodC* (C) and regulatory genes *nodD1* (D), *nodD2* (E) and transcriptional regulator of T3SS, *ttsI* (F). Data were normalized in relation to the endogenous control (16S rRNA). Values represent mean ± SD (n = 3). *P* values based on Tukey's test (*** $P < 0.001$).

3.4. Bradyrhizobium sp. SUTN9-2 copG$_1$ *is Involved in the Repression of T4SS Structural Genes traG*$_1$ *and trbE*$_1$

To understand the relationship of T4SS and *copG*$_1$ gene more clearly, the gene expression fold changes were examined. T4SS with *trbE*$_1$ and *traG*$_1$ genes showed high expression levels under non-symbiotic conditions when *copG*$_1$ was deleted (Figure 4A and 4B). These results indicated that *copG*$_1$ of SUTN9-2 may act as a suppressor of *trbE*$_1$ and *traG*$_1$ under non-symbiotic conditions. However, under mimicked symbiotic conditions with 20 µM genistein induction, the expression of the *trbE*$_1$ gene significantly decreased in Δ*copG*$_1$ compared to the wild type. The expression of the *traG*$_1$ gene did not differ in both the wild type and the Δ*copG*$_1$ (Figure 4C and 4D). However, it is noteworthy that under mimicked symbiosis conditions, CopG$_1$ can induce the expression of *trbE*$_1$ and *traG*$_1$, resulting in significantly higher levels than those observed under non-induction conditions. These results suggest that *copG*$_1$ might act as a synergistic regulator of the T4SS gene in SUTN9-2 under flavonoid induction (Figure 4C and 4D).

Preprints.org (www.preprints.org) | NOT PEER-REVIEWED | Posted: 8 May 2024 doi:10.20944/preprints202405.0436.v1

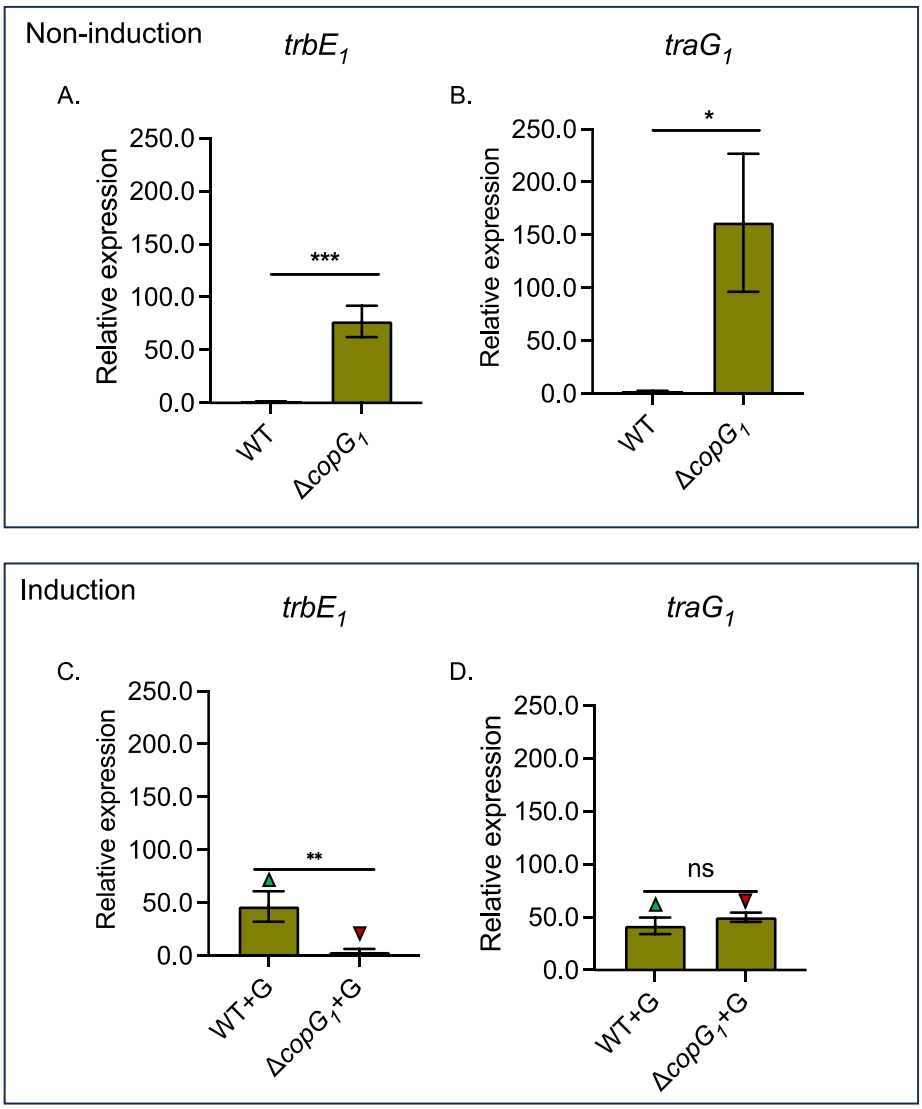

Figure 4. Relative expression of representatives T4SS structural genes, including *trbE*$_1$ (A, C), and *traG*$_1$ genes (B, D) in *Bradyrhizobium* sp. SUTN9-2 (WT) and Δ*copG*$_1$ with and without 20 μM genistein (G) induction. The 16S rRNA gene was used as an internal control. Values represent mean ± SD (n = 3). *P* values based on Student's t-test (ns $P > 0.05$, * $P < 0.05$, ** $P < 0.01$, *** $P < 0.001$). The green and red arrows represent a statistical increase and decrease, respectively, in gene expressions when comparing experiments with the presence and absence of genistein.

3.5. Effect of T4SS and copG$_1$ *on Secreted Protein Pattern after 48 h With Genistein Induction*

The secreted protein patterns of *Bradyrhizobium* sp. SUTN9-2, ΔT4SS$_1$, and Δ*copG*$_1$ with 20 μM genistein after 48 h induction were analyzed by SDS-PAGE. The results revealed distinct protein band patterns in the different conditions (Figure 5). The amino acid sequences of each selected band were examined using mass spectrometry (MS) with the MASCOT program. In the wild type with genistein induction (band 1) contain a protein matched with the T3SS translocon protein, NopX (27%), while this band was absent at the same position of ΔT4SS$_1$. Similarly, a protein band was observed in the wild type with genistein induction (band 6), a match was found with the T3SS host specificity protein, NopP (18%), this protein was not observed in ΔT4SS$_1$ (band 7) at the same position. While protein bands from the wild type (band 3) and ΔT4SS$_1$ (band 4) were found a protein matched with Dct; C_4-dicarboxylate ABC transporter (31%), but it was not observed in Δ*copG*$_1$ (band 5). Nevertheless, Δ*copG*$_1$ (band 5) was associated with amino acid ABC transporter substrate-binding protein glutamate/aspartate transporter subunit (38%).

 doi:10.20944/preprints202405.0436.v1

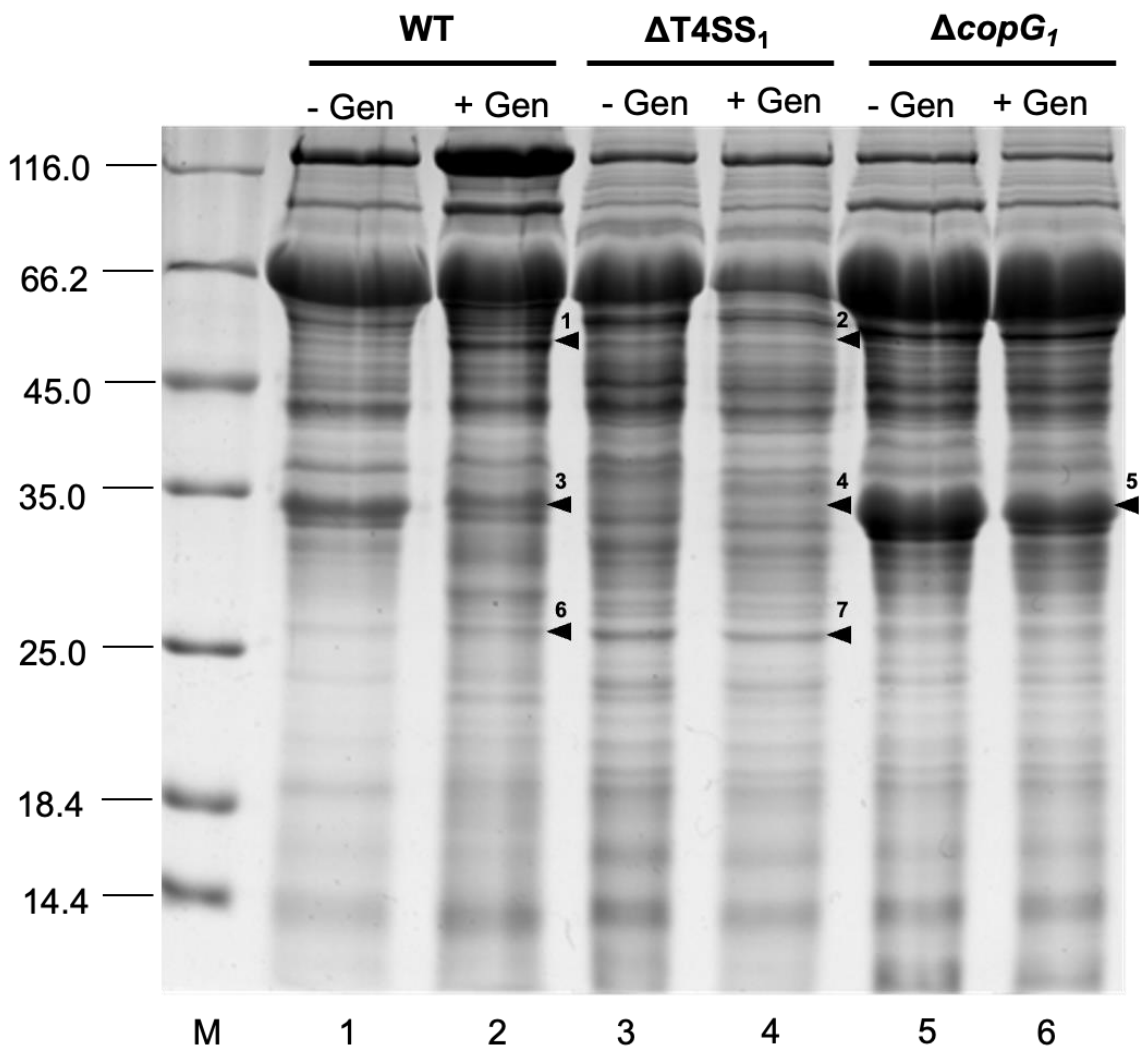

Figure 5. SDA-PAGE analysis of proteins secretion into the external medium of *Bradyrhizobium* sp. SUTN9-2 (WT), ΔT4SS$_1$, and Δ*copG*$_1$ with 20 μM genistein (+Gen) and without 20 μM genistein (-Gen) induction. Numbers on the left indicate molecular size markers in kilodaltons. The arrowhead indicates bands identified by mass spectrometry (MS) analysis of WT (1, 3, 6), ΔT4SS$_1$ (2, 4, 7), and Δ*copG*$_1$ (5).

qRT-PCR was performed to identify the gene expression of T3SS (*nopP* and *nopX*) and C$_4$-dicarboxylate transporter (*dct*), which was not in secreted protein from Δ*copG*$_1$. The results showed that the expression of T3Es (*nopP* and *nopX*) and C$_4$-dicarboxylate transporter (*dct*) under genistein induction was down-regulated in Δ*copG*$_1$ (Figure 6). This indicated that these genes required *copG*$_1$ to mediate the regulation under genistein induction.

 doi:10.20944/preprints202405.0436.v1

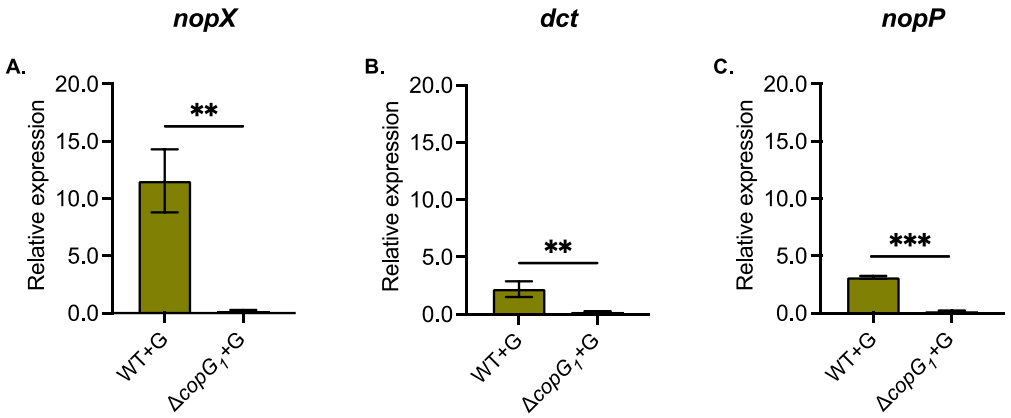

Figure 6. Relative expression of Nodulation outer protein X (*nopX*) (A), C4-dicarboxylate transporter (*dct*) (B), and *nopP* genes (C) in *Bradyhizobium* sp. SUTN9-2 (WT) and Δ*copG*1 under 20 μM genistein induction (+G). Data were normalized in relation to endogenous control (16S rRNA). Values represent mean ± SD (n = 3). *P* values based on Student's t-test (* P <0.05, ** P < 0.01,*** P < 0.001).

4. Discussion

At an early nodulation stage of *V. radiata* cv. SUT4, Δ*traG*1 and Δ*virD2*1 generated a high number of nodules with smaller size compared to the wild type (Figure 1I, 1M and 1Q-1R). The symbiosome space of Δ*traG*1 and Δ*virD2*1 infecting nodules revealed some dead cells that were not found in the wild type under confocal microscopy (Figure 1J and 1N). According to the findings, T4SS is beneficial in the early stages of symbiotic interaction between SUTN9-2 and legumes. Bradyrhizobia have a TraG/Trb operon on the chromosome in the symbiosis island that is similar to that of mesorhizobia based on the *traG* gene's phylogenetic and gene organization [15]. Beside the structural protein, various bacteria containing T4SS also identified ATPase/Coupling protein, VirD4/TraG and relaxase, VirD2 [20]. The *traG* is commonly found in conjugative plasmids that are responsible for horizontal gene transfer between bacteria. The *traG* gene required for encode T4SS component served as ATPase to generate energy during secretion [19]. In addition, TraG also act as a substrate receptor of T4SS called coupling protein, a substrate receptor that mediate the substrate such as effector proteins, DNA or DNA-protein complex through T4SS channel [7,10,41,42]. In the Pfam prediction, TraG protein was matched with Pfam family T4SS-DNA_transfer (PF02534), TrwB_AAD_bound (PF10412), and TraG-D_C (PF12696) (Figure S8A). The C-terminal of this protein is able to interact with the relaxosome, which is essential for DNA transfer and conjugation in bacteria [19,43,44]. In mesorhizobia, *traG* plays an important role in an early stage of infection, and its expression was observed during induction with root exudate and early nodules generated by *M. mediterraneum* Ca36^T. Corresponding to mesorhizobia, *traG*1 of SUTN9-2 may play a crucial role in the beginning of symbiotic interaction with legumes [7]. In *Agrobacterium*, VirD2 protein is a part of the relaxase family that plays a crucial in conjugating and mobilizing plasmids that are required for translocation and integration of T-strands into recipient plant cells [45,46]. The conjugative transfer of ICEMlSymR7A in *M. loti* R7A requires VirD2 relaxase to initiate the rolling-circle replication [47]. VirD21 of SUTN9-2 possesses a domain of unknown function (DUF), DUF3363, which is an uncharacterized protein (Figure S8B). Although Δ*virD2*1 had no effect on the number of nodules of *V. radiata* cv. SUT4, but the activity of nitrogen fixation was reduced (Figure 1S and 1T).

Nodules generated by Δ*virD2*1 showed many uninfected cells (Figure 1N and 1P). This finding showed that the communication between SUTN9-2 and the legume at the beginning of nodule organogenesis plays an important role in enhancing infection efficiency and nitrogenase activity after infection. These results strongly indicated that the *traG*1 and *virD2*1 genes may be necessary for symbiotic interaction during an early infection stage. Unlike Δ*traG*1 and Δ*virD2*1, Δ*copG*1 has an impact on the symbiotic interaction between SUTN9-2 and legumes because this mutant was unable to generate nodules with the tested plant (Figure 1E and 1G). Since, *copG*1 was located downstream

 doi:10.20944/preprints202405.0436.v1

of *traG*$_1$ and *virD2*$_1$ within the same cluster, it is assumed that *copG*$_1$ may share a common promoter with *traG*$_1$ and *virD2*$_1$. This observation was supported by the previous study, where T4SS complementation successfully restored nodule formation [15]. Several bacteria, such as *Pseudomonas aeruginosa* [48], *Streptococcus agalactiae* [38], *Vibrio cholerae* [49], *Bradyrhizobium* sp., and *Mesorhizobium* sp. contain the *copG* gene in their genomes [15]. This gene encodes CopG protein, a small transcriptional repressor containing a helix-turn-helix motif domain, which is similar to that of regulatory repressors such as Mnt, Arc, and MetJ in *Salmonella typhimurium* bacteriophage P22 and *Escherichia coli* [18,50,51]. The CopG protein was first discovered in streptococcal plasmid pMV158 as a transcriptional repressor that interacts with RepB to control the copy number of the plasmid [34,38,52]. In addition, copper resistance was also demonstrated to be influenced by CopG in *P. aeruginosa* and *V. cholerae* [48,49].

In SUTN9-2, the CopG$_1$ protein was classified as an uncharacterized conserved protein, while CopG$_2$ was annotated as the Pfam;RHH_1 domain (PF01402), which may serve as a transcriptional regulator within the CopG family (Figure S4) [34]. The removal of both *copG* genes in SUTN9-2 resulted in distinct nodulation efficiency. Even without a nodule generated by Δ*copG*$_1$, it can still infect plants because we could monitor both live and dead cells within plant tissues. Surprisingly, live cells were found mostly in the vascular bundle tissue, which is similar to how endophytic bacteria behave. These findings imply that *copG*$_1$ may be crucial for SUTN9-2 in protecting the survival of bacterial cells in the host plant. Bacteria can evolve and adapt to their environment through horizontal gene transfer, which is usually facilitated by conjugation. Conjugation is a significant biological process as it is the primary way to spread antibiotic resistance genes [53]. Integrative and conjugative elements (ICEs) are another essential mechanism that contributes to conjugation. ICEs are recognized as elements encoded for excision and transferred by conjugation and integration, regardless of the specific mechanisms involved [54]. The T4SS found in SUTN9-2 is classified as a *tra*/*trb* operon and is recognized for its crucial role in facilitating conjugal transfer. Although SUTN9-2 lacks a conjugation plasmid, ICE is still present on the chromosome. The genes encoding the T4SS$_1$ cluster are presented in this ICE, which is an alternative mechanism of genetic exchange in this bacterial strain [15]. In order to study the impaired nodulation phenotype of Δ*copG*$_1$ in *V. radiata* cv. SUT4, we analyzed the expression of *nod* genes with and without genistein induction. Common *nod* genes in SUTN9-2 including *nodA* and *nodC* genes were not expressed even with a lack of *copG*$_1$ under flavonoid induction condition, but it did not affect *nodB* expression. Additionally, *copG*$_1$ acts as a stimulator for *nodD1* and *nodD2*, which are the primary transcription factors responsible for NF production. In addition to *nod* genes, the expression level of *ttsI*, which was not determined in Δ*copG*$_1$. TtsI protein is a transcriptional regulator (previously called *y4xI*) is activated by flavonoids and NodD1 that bind to conserved sequences called *tts-boxes* [40,55,56]. This protein controlled the genes responsible for T3SS synthesis and effector protein secretion which have an effect for symbiosis interaction between rhizobium-legumes interaction depends on plant host [6,57]. During symbiotic interaction, SUTN9-2 required *copG*$_1$ to mediate the expression of *nod* genes and *ttsI* under flavonoid induction. These results indicate that CopG$_1$ may positively mediate the expression of *nod* genes via NodD activation before stimulating NF production, nodule organogenesis and T3SS. Furthermore, *copG*$_1$ plays a role as a repressor in T4SS gene expression, suppressing *trbE* and *traG* gene expression under flavonoid stimulation (Figure 4C and 4D). In contrast, these genes were not affected by flavonoids in the absence of the *copG*$_1$ gene.

The protein expression profiles of SUTN9-2, ΔT4SS$_1$ and Δ*copG*$_1$ with genistein treatment were analyzed by SDS-PAGE. The results revealed distinct protein band patterns in the different conditions (Figure 5). Δ*copG*$_1$ exhibited a deficiency in producing nodules in various plant species and a striking increase in protein expression compared to the wild type. According to the analysis of *copG*$_1$ domain protein (Figure S4), *CopG*$_1$ was predicted to be a transcriptional regulator which might play a role in the regulation of gene expression. The Δ*copG*$_1$ lane appears to have much more protein intensity overall because the proportion of protein in this lane might be less than other lanes. So, 10 µg might be shown higher band intensity. A comparative proteomic analysis of the whole secretome should be conducted further to identify additional target proteins involved in this interaction. It was

 doi:10.20944/preprints202405.0436.v1

found that several proteins were secreted, but the C_4-dicarboxylate transport system (*dct*) protein was not identified in Δ*copG*$_1$ and this result was corresponded to the down-regulated of *dct* gene quantified by qRT-PCR (Figure 6). The *dct* gene play a crucial role for symbiosis in numerous rhizobia [58]. For example, the *dct* mutant of *S. meliloti* and *R. trifolii* can generate ineffective nodules with the host legume [59,60]. Besides the *dct* gene, there are other genes that are expressed in the same pattern, including *nopX* and *nopP*, which are also essential for symbiosis (Figure 6). NopX is a component of T3SS as a translocation pore (translocon) apparatus that is important for host-specific interaction between the rhizobium and host plant. The NGRΔ*nopX* has a significant effect on the nodule number because this mutant forms fewer nodules in all plant species tested, including *Flemingia congesta*, *Tephrosia vogelii*, *Pachyrhizus tuberosus,* and *Lablab purpureus* [61]. NopP is a T3SS effector protein that is phosphorylated by plant kinases [62]. A lack of NopP in *Rhizobium* sp. NGR234 reduces the capacity of nodule organogenesis in tropical legumes. This indicates a positive effect of NopP on symbiosis [61]. NopP of *B. diazoefficiens* USDA122 is necessary and causes Rj2-dependent incompatibility [63]. The T3SS of SUTN9-2 has no impact on the symbiotic relationship with *V. radiata* [11]. However, based on the protein secretion results of T3Es (NopP and NopX) and *nodD* gene expression, it is evident that *copG*$_1$ regulates the function of *nodD* and T3SS. Previous reports indicated that *nodD* controls the function of *nod* cluster by binding to the nod box region. Similarly, *nodD* can regulate the T3SS function by binding to *ttsI* [55]. Therefore, the results of this experiment confirm that CopG$_1$ controls the function of *nodD*, influencing the expression of the *nod* cluster genes and T3SS. Perhaps, CopG$_1$ is a crucial factor in the early stage of legume and SUTN9-2 communication. It is plausible that the regulatory system governing the expression of *nod* genes does not solely depend on the interaction between flavonoids and NodD. Another factor, CopG$_1$, also collaborates with flavonoids and NodD in regulating the expression of *nod* genes and T3SS. Carbon and nitrogen metabolism are the primary mechanisms that are necessary for the exchange of nutrients between plant and bacteria partners. The proteins secreted from Δ*copG*$_1$ matched with the periplasmic binding proteins of the glutamate/aspartate ABC transporter. Glutamate is a significant contributor to the total metabolite content, which plays an essential role in nitrogen metabolism, amino acid metabolism, transamination, and carbon sources [64,65]. During symbiosis, the main carbon source utilized by rhizobia is C_4-dicarboxylic acid [66,67]. In the mimicked symbiotic conditions, Δ*copG*$_1$ lost the ability to establish symbiotic interaction. Thereafter, the increasing of glutamate/aspartate ABC transporter may promote carbon and nitrogen uptake to support bacterial cell survival, but it is not necessary for symbiotic interaction. This again suggests that *copG*$_1$ may act as a regulator of *nodD* and T4SS gene expression under symbiosis conditions.

5. Conclusions

The T4SS$_1$ containing *copG*$_1$, *traG*$_1$, and *virD2*$_1$ has beneficial effects on symbiotic interactions with diverse legumes. The deletion of each gene in a unique cluster showed a distinctive effect on symbiosis. The early stage of infection and nodulation is influenced by *traG*$_1$ and *virD2*$_1$, while nodulation with legume hosts was not efficient in the absence of *copG*$_1$. While, *copG*$_1$ is necessary for nodulation, the Δ*copG*$_2$ results in reduced nitrogenase activity, despite maintaining high nodule numbers. This underscores the essential role of *copG*$_2$ in nitrogenase efficiency. Overall, both *copG*$_1$ and *copG*$_2$ genes play crucial roles in the symbiotic relationship between SUTN9-2 and legume plants, contributing to effective nitrogen fixation during symbiosis. The expression of nodulation (*nod*) genes including common *nodA*, *nodC*, *nodD1,* and *nodD2* and *ttsI* were not detected with and without genistein induction in Δ*copG*$_1$, while the T4SS genes in Δ*copG*$_1$ were highly expressed in non-induction conditions. Interestingly, the absence of *copG*$_1$ with the induction of flavonoid led to a low expression level of T4SS genes. The results suggest that *copG*$_1$ may play an important role in nodulation, which is a crucial for the symbiotic interaction between *Bradyrhizobium* sp. SUTN9-2 and legumes. Additionally, *copG*$_1$ served as a suppressor of T4SS genes under non-induction conditions and was required to stimulate the expression of T4SS genes through flavonoid induction. *copG*$_1$ also acted as a suppressor of secreted protein under flavonoid induction conditions. In addition, a lack of *copG*$_1$ led to suppressed expression of *nopX*, *nopP*, and *dct*, which are important for infection and nodulation

during symbiosis. Thus, *copG*$_1$ is most likely responsible for regulation via functions in T3SS, *nodD* regulation, and the carbon and nitrogen exchange systems, which are significant for SUTN9-2 during symbiosis.

Supplementary Materials: The following supporting information can be downloaded at: www.mdpi.com/xxx/s1, Figure S1: title; Table S1: title; Video S1: title.

Acknowledgments: This work was supported by (i) The Royal Golden Jubilee Ph.D. Programme (RGJ) scholarship under the Thailand Research Fund (TRF), (ii) Suranaree University of Technology (SUT), National Science, Research, and Innovation Fund (NSRF), (iii) the NSRF via the Program Management Unit for Human Resources & Institutional Development, Research, and Innovation (grant number B16F640113), (iv) the Office of the Permanent Secretary of the Ministry of Higher Education, Science, Research, and Innovation, and (v) National Research Council of Thailand (NRTC) and Suranaree University of Technology (grant number N42A650322).

References

1. Dénarié, J.; Debellé, F.; Promé, J.-C. *Rhizobium* lipo-chitooligosaccharide nodulation factors: signaling molecules mediating recognition and morphogenesis *Annu. Rev. Biochem.* **1996**, *65*, 503–535.
2. Hanin, M.; Jabbouri, S.; Quesada-Vincens, D.; Freiberg, C.; Perret, X.; Promé, J. -C.; Broughton, W.J.; Fellay, R. Sulphation of *Rhizobium* sp. NGR234 Nod-Factors is dependent on *noeE*, a new host-specificity gene. *Mol. Microbiol.* **1997**, *24*, 1119–1129.
3. Fauvart, M.; Michiels, J. Rhizobial secreted proteins as determinants of host specificity in the *rhizobium*-legume symbiosis. *FEMS Microbiol. Lett.* **2008**, *285*, 1-9.
4. Nelson, M.S.; Sadowsky, M.J. Secretion systems and signal exchange between nitrogen-fixing rhizobia and legumes. *Front. Plant Sci.* **2015**, *6*, 491.
5. Jiménez-Guerrero, I.; Medina, C.; Vinardell, J.M.; Ollero, F.J.; López-Baena, F.J. The rhizobial type 3 secretion system: The Dr. Jekyll and Mr. Hyde in the *rhizobium*–legume symbiosis. *Int. J. Mol. Sci.* **2022**, *23*, 11089.
6. Songwattana, P.; Chaintreuil, C.; Wongdee, J.; Teulet, A.; Mbaye, M.; Piromyou, P.; Gully, D.; Fardoux, J.; Zoumman, A.M.A.; Camuel, A.; et al. Identification of type III effectors modulating the symbiotic properties of *Bradyrhizobium vignae* strain ORS3257 with various *Vigna* species. *Sci. Rep.* **2021**, *11*, 4874.
7. Paço, A.; Da-Silva, J.R.; Eliziário, F.; Brígido, C.; Oliveira, S.; Alexandre, A. *traG* gene is conserved across *Mesorhizobium* spp. able to nodulate the same host plant and expressed in response to root exudates. *BioMed Res. Int.* **2019**, *2019*, 3715271.
8. Salinero-Lanzarote, A.; Pacheco-Moreno, A.; Domingo-Serrano, L.; Durán, D.; Ormeño-Orrillo, E.; Martínez-Romero, E.; Albareda, M.; Palacios, J.M.; Rey, L. Type VI secretion system of *Rhizobium etli* Mim1 has a positive effect in symbiosis. *FEMS Microbiol. Ecol.* **2019**, *95*, fiz054.
9. Tighilt, L.; Boulila, F.; De Sousa, B.F.S.; Giraud, E.; Ruiz-Argüeso, T.; Palacios, J.M.; Imperial, J.; Rey, L. The *Bradyrhizobium* sp. LmicA16 type VI secretion system is required for efficient nodulation of *Lupinus* spp. *Microb. Ecol.* **2022**, *84*, 844–855.
10. Fronzes, R.; Christie, P.J.; Waksman, G. The structural biology of type IV secretion systems. *Nat. Rev. Microbiol.* **2009**, *7*, 703–714.
11. Piromyou, P.; Songwattana, P.; Teamtisong, K.; Tittabutr, P.; Boonkerd, N.; Tantasawat, P.A.; Giraud, E.; Göttfert, M.; Teaumroong, N. Mutualistic co-evolution of T3SSs during the establishment of symbiotic relationships between *Vigna radiata* and bradyrhizobia. *MicrobiologyOpen* **2019**, *8*, e00781.
12. Kaneko, T.; Maita, H.; Hirakawa, H.; Uchiike, N.; Minamisawa, K.; Watanabe, A.; Sato, S. Complete genome sequence of the soybean symbiont *Bradyrhizobium japonicum* strain USDA6^T. *Genes* **2011**, *2*, 763–787.
13. Okazaki, S.; Noisangiam, R.; Okubo, T.; Kaneko, T.; Oshima, K.; Hattori, M.; Teamtisong, K.; Songwattana, P.; Tittabutr, P.; Boonkerd, N.; et al. Genome analysis of a novel *Bradyrhizobium* sp. DOA9 carrying a symbiotic plasmid. *PLOS ONE* **2015**, *10*, e0117392.
14. Cytryn, E.J.; Jitacksorn, S.; Giraud, E.; Sadowsky, M.J. Insights learned from pBTAi1, a 229-Kb accessory plasmid from *Bradyrhizobium* sp. strain BTAi1 and prevalence of accessory plasmids in other *Bradyrhizobium* sp. strains. *ISME J.* **2008**, *2*, 158–170.
15. Wangthaisong, P.; Piromyou, P.; Songwattana, P.; Wongdee, J.; Teamtaisong, K.; Tittabutr, P.; Boonkerd, N.; Teaumroong, N. The type IV secretion system (T4SS) mediates symbiosis between *Bradyrhizobium* sp. SUTN9-2 and legumes. *Appl. Environ. Microbiol.* **2023**, *89*, e00040-23.

16. Zhang, Y.F.; Wang, E.T.; Tian, C.F.; Wang, F.Q.; Han, L.L.; Chen, W.F.; Chen, W.X. *Bradyrhizobium elkanii* , *Bradyrhizobium yuanmingense* and *Bradyrhizobium japonicum* are the main rhizobia associated with *Vigna unguiculata* and *Vigna radiata* in the subtropical region of China. *FEMS Microbiol. Lett.* **2008**, *285*, 146–154.
17. Albareda, M.; Rodríguez-Navarro, D.N.; Temprano, F.J. Soybean inoculation: dose, N fertilizer supplementation and rhizobia persistence in sSoil. *Field Crops Res.* **2009**, *113*, 352–356.
18. Costa, M.; Solà, M.; Del Solar, G.; Eritja, R.; Hernández-Arriaga, A.M.; Espinosa, M.; Gomis-Rüth, F.X.; Coll, M. Plasmid transcriptional repressor CopG oligomerises to render helical superstructures unbound and in complexes with oligonucleotides. *J. Mol. Biol.* **2001**, *310*, 403–417.
19. Schröder, G.; Krause, S.; Zechner, E.L.; Traxler, B.; Yeo, H.-J.; Lurz, R.; Waksman, G.; Lanka, E. TraG-like proteins of DNA transfer systems and of the *Helicobacter pylori* type IV secretion system: inner membrane gate for exported substrates? *J. Bacteriol.* **2002**, *184*, 2767–2779.
20. Tegtmeyer, N.; Linz, B.; Yamaoka, Y.; Backert, S. Unique TLR9 activation by Helicobacter pylori depends on the Cag T4SS, but not on VirD2 relaxases or VirD4 coupling proteins. *Curr. Microbiol.* **2022**, *79*, 121.
21. Sadowsky, M.J.; Tully, R.E.; Cregan, P.B.; Keyser, H.H. Genetic Diversity in *Bradyrhizobium japonicum* serogroup 123 and its relation to genotype-specific nodulation of soybean. *Appl. Environ. Microbiol.* **1987**, *53*, 2624–2630.
22. Ditta, G.; Stanfield, S.; Corbin, D.; Helinski, D.R. Broad host range DNA cloning system for Gram-negative bacteria: construction of a gene bank of *Rhizobium meliloti*. *Proc. Natl. Acad. Sci.* **1980**, *77*, 7347–7351.
23. Tsai, J.-W.; Alley, M.R.K. Proteolysis of the McpA chemoreceptor does not require the *Caulobacter* major chemotaxis operon. *J. Bacteriol.* **2000**, *182*, 504–507.
24. Blondelet-Rouault, M.-H.; Weiser, J.; Lebrihi, A.; Branny, P.; Pernodet, J.-L. Antibiotic resistance gene cassettes derived from the π interposon for use in *E. coli* and *Streptomyces*. *Gene* **1997**, *190*, 315–317.
25. Muyzer, G.; De Waal, E.C.; Uitterlinden, A.G. Profiling of complexmicrobial populations by denaturing gradient gel electrophoresis analysis of polymerase chain reaction-amplified genes coding for 16S rRNA. *Appl. Environ. Microbiol.* **1993**, *59*, 695–700.
26. Teamtisong, K.; Songwattana, P.; Noisangiam, R.; Piromyou, P.; Boonkerd, N.; Tittabutr, P.; Minamisawa, K.; Nantagij, A.; Okazaki, S.; Abe, M.; et al. Divergent *nod*-containing *Bradyrhizobium* sp. DOA9 with a megaplasmid and its host range. *Microbes Environ.* **2014**, *29*, 370–376.
27. Ehrhardt, D.; Atkinson, E.; Long depolarization of alfalfa root hair membrane potential by *Rhizobium meliloti* Nod factors. *Science* **1992**, *256*, 998–1000, doi:10.1126/science.10744524.
28. Renier, S.; Hébraud, M.; Desvaux, M. Molecular biology of surface colonization by *Listeria monocytogenes* : an additional facet of an opportunistic Gram-positive foodborne pathogen. *Environ. Microbiol.* **2011**, *13*, 835–850.
29. Somasegaran, P.; Hoben, H.J. *Handbook for rhizobia*; Springer New York: New York, NY, 1994; ISBN 978-1-4613-8377-2.
30. Phimphong, T.; Sibounnavong, P.; Phommalath, S.; Wongdee, J.; Songwattana, P.; Piromyou, P.; Greetatorn, T.; Boonkerd, N.; Tittabutr, P.; Teaumroong, N. Selection and evaluation of *Bradyrhizobium* inoculum for peanut, *Arachis hypogea* production in the Lao People's Democratic Republic. *J. Appl. Nat. Sci.* **2023**, *15*, 137–154.
31. Bradford, M. A rapid and sensitive method for the quantitation of microgram quantities of protein utilizing the principle of protein-dye binding. *Anal. Biochem.* **1976**, *72*, 248–254.
32. Laemmli, U.K. Cleavage of structural proteins during the assembly of the head of bacteriophage T4. *Nature* **1970**, *227*, 680–685.
33. Haag, A.F.; Baloban, M.; Sani, M.; Kerscher, B.; Pierre, O.; Farkas, A.; Longhi, R.; Boncompagni, E.; Hérouart, D.; Dall'Angelo, S.; et al. Protection of *Sinorhizobium* against host cysteine-rich antimicrobial peptides is critical for symbiosis. *PLoS Biol.* **2011**, *9*, e1001169.
34. Acebo, P.; García De Lacoba, M.; Rivas, G.; Andreu, J.M.; Espinosa, M.; Solar, G.D. Structural features of the plasmid pMV158-encoded transcriptional repressor CopG, a protein sharing similarities with both helix-turn-helix and β-sheet DNA binding proteins. *Proteins Struct. Funct. Genet.* **1998**, *32*, 248–261.
35. Vallenet, D.; Calteau, A.; Dubois, M.; Amours, P.; Bazin, A.; Beuvin, M.; Burlot, L.; Bussell, X.; Fouteau, S.; Gautreau, G.; et al. MicroScope: an integrated platform for the annotation and exploration of microbial gene functions through genomic, pangenomic and metabolic comparative analysis. *Nucleic Acids Res.* **2020**, gkz926.
36. Letunic, I.; Khedkar, S.; Bork, P. SMART: recent updates, new developments and status in 2020. *Nucleic Acids Res.* **2021**, *49*, D458–D460.
37. Paysan-Lafosse, T.; Blum, M.; Chuguransky, S.; Grego, T.; Pinto, B.L.; Salazar, G.A.; Bileschi, M.L.; Bork, P.; Bridge, A.; Colwell, L.; et al. InterPro in 2022. *Nucleic Acids Res.* **2023**, *51*, D418–D427.

38. Gomis-Ruth, F.X. The structure of plasmid-encoded transcriptional repressor CopG unliganded and bund to its operator. *EMBO J.* **1998**, *17*, 7404–7415.
39. Heidstra, R.; Bisseling, T. Nod factor-induced host responses and mechanisms of Nod factor perception. *New Phytol.* **1996**, *133*, 25–43.
40. Marie, C.; Deakin, W.J.; Ojanen-Reuhs, T.; Diallo, E.; Reuhs, B.; Broughton, W.J.; Perret, X. TtsI, a key regulator of *Rhizobium* species NGR234 is required for type III-dependent protein secretion and Synthesis of Rhamnose-Rich Polysaccharides. *Mol. Plant-Microbe Interactions.* **2004**, *17*, 958–966, doi:10.1094/MPMI.2004.17.9.958.
41. Cascales, E.; Atmakuri, K.; Sarkar, M.K.; Christie, P.J. DNA Substrate-Induced Activation of the Agrobacterium VirB/VirD4 Type IV Secretion System. *J. Bacteriol.* **2013**, *195*, 2691–2704, doi:10.1128/JB.00114-13.
42. Christie, P.J.; Whitaker, N.; González-Rivera, C. Mechanism and structure of the bacterial type IV secretion systems. *Biochim. Biophys. Acta BBA - Mol. Cell Res.* **2014**, *1843*, 1578–1591.
43. Gunton, J.E.; Gilmour, M.W.; Baptista, K.P.; Lawley, T.D.; Taylor, D.E. Interaction between the co-inherited TraG coupling protein and the TraJ membrane-associated protein of the H-plasmid conjugative DNA transfer system resembles chromosomal DNA translocases. *Microbiology* **2007**, *153*, 428–441.
44. Lu, J.; Wong, J.J.W.; Edwards, R.A.; Manchak, J.; Frost, L.S.; Glover, J.N.M. Structural basis of specific TraD-TraM recognition during F plasmid-mediated bacterial conjugation. *Mol. Microbiol.* **2008**, *70*, 89–99.
45. Byrd, D.R.; Matson, S.W. Nicking by transesterification: the reaction catalysed by a relaxase. *Mol. Microbiol.* **1997**, *25*, 1011–1022.
46. Van Kregten, M.; Lindhout, B.I.; Hooykaas, P.J.J.; Van Der Zaal, B.J. *Agrobacterium* -mediated T-DNA transfer and integration by minimal VirD2 consisting of the relaxase domain and a type IV secretion system translocation signal. *Mol. Plant-Microbe Interactions*. **2009**, *22*, 1356–1365.
47. Ramsay, J.P.; Sullivan, J.T.; Stuart, G.S.; Lamont, I.L.; Ronson, C.W. Excision and transfer of the *Mesorhizobium loti* R7A symbiosis island requires an integrase IntS, a novel recombination directionality factor RdfS, and a putative relaxase RlxS. *Mol. Microbiol.* **2006**, *62*, 723–734.
48. Hausrath, A.C.; Ramirez, N.A.; Ly, A.T.; McEvoy, M.M. The bacterial copper resistance protein CopG contains a cysteine-bridged tetranuclear copper cluster. *J. Biol. Chem.* **2020**, *295*, 11364–11376.
49. Marrero, K.; Sánchez, A.; González, L.J.; Ledón, T.; Rodríguez-Ulloa, A.; Castellanos-Serra, L.; Pérez, C.; Fando, R. Periplasmic proteins encoded by VCA0261–0260 and VC2216 genes together with *copA* and *cueR* products are required for copper tolerance but not for virulence in *Vibrio cholerae*. *Microbiology* **2012**, *158*, 2005–2016.
50. Breg, J.N.; Van Opheusden, J.H.J.; Burgering, M.J.M.; Boelens, R.; Kaptein, R. Structure of Arc repressor in solution: evidence for a family of β-sheet DNA-binding proteins. *Nature* **1990**, *346*, 586–589.
51. Somers, W.S.; Phillips, S.E.V. Crystal structure of the Met repressor–operator complex at 2.8 Å resolution reveals DNA recognition by β-strands. *Nature* **1992**, *359*, 387–393.
52. del Solar, G.; Hernández-Arriaga, A.M.; Gomis-Rüth, F.X.; Coll, M.; Espinosa, M. A Genetically economical family of plasmid-encoded transcriptional repressors involved in control of plasmid copy number. *J. Bacteriol.* **2002**, *184*, 4943–4951, doi:10.1128/JB.184.18.4943-4951.2002.
53. Guglielmini, J.; Quintais, L.; Garcillán-Barcia, M.P.; de la Cruz, F.; Rocha, E.P.C. The repertoire of ICE in prokaryotes underscores the unity, diversity, and ubiquity of conjugation. *PLoS Genet.* **2011**, *7*, e1002222.
54. Bellanger, X.; Payot, S.; Leblond-Bourget, N.; Guédon, G. Conjugative and mobilizable genomic islands in bacteria: evolution and diversity. *FEMS Microbiol. Rev.* **2014**, *38*, 720–760.
55. Krause, A.; Doerfel, A.; Göttfert, M. Mutational and transcriptional analysis of the type III secretion system of *Bradyrhizobium japonicum*. *Mol. Plant-Microbe Interactions.* **2002**, *15*, 1228–1235.
56. Kobayashi, H.; Graven, Y.N.; Broughton, W.J.; Perret, X. Flavonoids induce temporal shifts in gene-expression of *nod* -box controlled loci in *Rhizobium* sp. NGR234. *Mol. Microbiol.* **2004**, *51*, 335–347.
57. Teulet, A.; Camuel, A.; Perret, X.; Giraud, E. Theversatile roles of type III secretion systems in *Rhizobium*-legume symbioses. *Annu. Rev. Microbiol.* **2022**, *76*, 45–65.
58. Yurgel, S.N.; Kahn, M.L. Dicarboxylate transport by rhizobia. *FEMS Microbiol. Rev.* **2004**, *28*, 489–501.
59. Ronson, C.W.; Lyttleton, P.; Robertson, J.G. C_4 -dicarboxylate transport mutants of *Rhizobium trifolii* form ineffective nodules on *Trifolium Repens*. *Proc. Natl. Acad. Sci.* **1981**, *78*, 4284–4288.
60. Yurgel, S.N.; Kahn, M.L. *Sinorhizobium meliloti dctA* mutants with partial ability To transport dicarboxylic acids. *J. Bacteriol.* **2005**, *187*, 1161–1172.
61. Marie, C.; Deakin, W.J.; Viprey, V.; Kopciñska, J.; Golinowski, W.; Krishnan, H.B.; Perret, X.; Broughton, W.J. Characterization of Nops, nodulation outer proteins, secreted via the type III secretion system of NGR234. *Mol. Plant-Microbe Interactions.* **2003**, *16*, 743–751.

 doi:10.20944/preprints202405.0436.v1

62. Bartsev, A.V.; Boukli, N.M.; Deakin, W.J.; Staehelin, C.; Broughton, W.J. Purification and phosphorylation of the effector protein NopL from *Rhizobium* sp. NGR234. *FEBS Lett.* **2003**, *554*, 271–274.
63. Sugawara, M.; Takahashi, S.; Umehara, Y.; Iwano, H.; Tsurumaru, H.; Odake, H.; Suzuki, Y.; Kondo, H.; Konno, Y.; Yamakawa, T.; et al. ariation in bradyrhizobial NopP effector determines symbiotic incompatibility with Rj2-soybeans via effector-triggered immunity. *Nat. Commun.* **2018**, *9*, 3139.
64. Streeter, J.G. Effect of nitrate on the organic acid and amino acid composition of legume nodules. *Plant Physiol.* **1987**, *85*, 774–779.
65. Forde, B.G.; Lea, P.J. Glutamate in plants: metabolism, regulation, and signalling. *J. Exp. Bot.* **2007**, *58*, 2339–2358.
66. Finan, T.M.; Wood, J.M.; Jordan, D.C. Symbiotic properties of C_4-dicarboxylic acid transport mutants of *Rhizobium leguminosarum*. *J. Bacteriol.* **1983**, *154*, 1403–1413.
67. Jording, D.; Sharma, P.K.; Schmidt, R.; Engelke, T.; Uhde, C.; Pühler, A. Regulatory aspects of the C_4-dicarboxylate transport in Rhizobium meliloti: transcriptional activation and dependence on effectave symbiosis. *J. Plant Physiol.* **1993**, *141*, 18–27.